Journal of Non-Crystalline Solids 354 (2008) 4359–4362

Contents lists available at ScienceDirect

Journal of Non-Crystalline Solids

journal homepage: www.elsevier.com/locate/jnoncrysol

Nanocrystallization and structure of $Fe_{78.5}Ni_{1.0}Mo_{0.5}Si_{6.0}B_{14.0}$ amorphous alloy

L. Bednarska [a,*], S. Mudry [a], M. Kovbuz [a], B. Kotur [a], O. Hertsyk [a], G. Haneczok [b], M. Karolus [b]

[a] Ivan Franko National University of Lviv, Kyryla and Mefodiya Strasse 6, UA-79005 Lviv, Ukraine
[b] Institute of Materials Science, University of Silesia, Bankowa Strasse 12, 40-007 Katowice, Poland

ARTICLE INFO

Article history:
Available online 16 August 2008

PACS:
68.55.−a
68.60.Dv
68.49.Jk
68.03.Fg

Keyword:
Alloys

ABSTRACT

The effect of Ni and Mo alloying additions on crystallization of an Fe–Si–B based amorphous alloy was studied by applying various experimental techniques – DSC, XRD and TEM. It was shown that both alloying additions Ni and Mo change the crystallization temperature as well as the activation energy of primary crystallization. The phases formed during primary crystallization for the $Fe_{80}Si_6B_{14}$ and $Fe_{78.5}Ni_1Mo_{0.5}Si_6B_{14}$ alloys were the same, however the morphologies were significantly different. The addition of 1.0 at.% of Ni and 0.5 at.% Mo changed the crystallization mechanism and the type of formed phases. Such additions also resulted in formation of nanocrystals. The kinetic and thermodynamic characteristics of annealed specimens of amorphous metallic $Fe_{80}Si_6B_{14}$ and $Fe_{78.5}Ni_1Mo_{0.5}Si_6B_{14}$ alloys were established. These characteristics were determined based on measurements of instantaneous changes of electrical strength. It was shown that the method of electromotive force measurements was more sensitive to structural changes and the phase composition of amorphous metallic electrodes in comparison with the X-ray method.

1. Introduction

Nanocrystallization processes taking place in Fe–Si–B amorphous metallic alloys (AMA) with various alloying additions were examined in detail in [1–3]. The influence of Cu and Nb additions on nanocrystallization processes was studied in [4,5], where an optimal concentration range of Cu and Nb in order to obtain materials with the best magnetic and electric conductivity properties was determined. The addition of Mo to AMA changes the magnetic properties, particularly the magnetostriction coefficient. For AMA like Fe–Si–B the crystallization kinetics is usually examined with the Kissinger formulae as well as the Avraami approach as was done in [6]. The electrochemical properties (corrosion current and potential) were studied in [7–10]. In should be emphasized that these studies permit only to estimate the crystallization kinetics parameters. The aim of this work is to obtain the nanocrystal formation rate, i.e. the activation energy E_a of nanocrystallization, and the cell parameters of the newly formed nanocrystals. It is known that physical as well as chemical properties of amorphous metallic alloys depend on the chemical short-range order describing different kind of atoms distribution, and also on the topological structure which commonly differs from random atomic distribution [11,12]. Evidently, these AMA properties of the structure lead to the appearance of microgalvanic cells on the AMA surface and consequently the electrochemical properties on the surface show a violent change upon the initial stage of crystallization. Taking into account the above, we intend to establish a correlation between the results of X-ray diffraction studies and electrochemical repercussion on structure changes due to thermal treatment. The thermodynamic characteristic (ΔG^0) calculated from the results on momentary fixation of electromotive force for $Fe_{80}Si_6B_{14}$ and the $Fe_{78}Ni_1Mo_{0.5}Si_6B_{14}$ amorphous metallic alloys were used in order to predict the structure change at thermal treatment.

2. Experimental procedure

The examined amorphous alloys $Fe_{80}Si_6B_{14}$ and $Fe_{78}Ni_1Mo_{0.5}Si_6B_{14}$ were obtained by the melt spinning method in the form of ribbons about 20 μm and 25 mm wide and thick, respectively. All the alloys were checked (X-ray diffraction method) and confirmed to be amorphous in the as received condition.

In order to study the crystallization kinetics for the as quenches samples differential scanning calorimetry (DSC, Perkin–Elmer Pyris 1), measurements with various heating rates (5, 10 and 20 K/min) were used. The obtained data were evaluated by applying the Pyris standard program. The DSC peaks positions were used for determining the annealing temperatures of the amorphous melt-spun ribbons. The samples were encapsulated in evacuated quartz tubes and annealed with the heating rate of 20 K/min up to the following temperatures: 670, 760, 786, 800, 815, 828 K.

The structural changes taking place in the annealed samples were examined by applying the X-ray diffraction method (X'-Pert Philips PW 3040 diffractometer, Cu K_α radiation with graphite

* Corresponding author.
E-mail address: L_Bednarska@franko.lviv.ua (L. Bednarska).

0022-3093/$ - see front matter © 2008 Published by Elsevier B.V.
doi:10.1016/j.jnoncrysol.2008.06.051

monochromator on a reflected beam, 2θ range: 10–140°, scanning step 0.04°). The experimental data were analyzed using the Rietveld method (standard FullProf program) [13].

The influence of isothermal annealing (in argon atmosphere) on the structural changes of AMA was investigated by applying the instantaneous fixed electromotive force (EMF) method. A polished AMA-electrode and a polished $Fe_{cryst.}$-electrode were immersed concurrently and immediately in a deaerated solution $Fe(NO_3)_3$. The EMF in element Fe-AMA$|Fe(NO_3)_3 \times 9H_2O + aq|Fe_{cryst.}$ was studied using an IMP88PC-R potentio-state. The surface state of the tested electrode was estimated also by measurements of the open circle potential (E_F) and the open circle current (Fig. 4) [14,15].

In order to confirm (or not) the conclusions established by DSC and X-ray techniques high-resolution electron microscopy (HREM, JEM 3010) observations were used.

3. Result and discussion

Fig. 1 shows DSC curves obtained for the $Fe_{78.5}Ni_1Mo_{0.5}Si_6B_{14}$ amorphous alloy at heating rates of 5, 10, 20 K/min. It can be seen that there are two-stages in the crystallization process as two exothermic DSC peaks are observed. The shift of the DSC peaks to a higher temperature with the increasing heating rate proves that the corresponding reaction-rate constants are temperature dependent. The difference between two peaks positions increases with the increasing heating rate which indicates that the activation energies of the two crystallization processes (primary and secondary) corresponding to the exothermic peaks are different. For samples with double Ni and Mo doping two peaks were observed which suggests that in addition to primary and secondary crystallization, processes such as decomposition of phase Fe_3B to phase Fe_2B and α-Fe also occurred at higher temperatures.

The apparent activation energy of each crystallization step can be determined by applying Kissinger's formula, which can be written as

$$\ln\left(\frac{T_x^2}{V}\right) = \frac{E_a}{RT_x} + \text{const}, \quad (1)$$

where T_x is the DSC peak temperature, V is the heating rate, R is the gas constant and E_a is the apparent activation energy. Fig. 2 shows Kissinger's plots for each peak presented in Fig. 1.

The obtained values are listed in Table 1, where the DSC peak temperatures are also included. The activation energies determined for the $Fe_{78.5}Ni_{1.0}Mo_{0.5}Si_{6.0}B_{14.0}$ alloy are 440 ± 50 kJ/mol and 510 ± 60 kJ/mol for the first and the second peak, respectively. For the base alloy $Fe_{80}Si_6B_{14}$ these values are significantly smaller, i.e. it is 380 kJ/mol for the first peak and 340 kJ/mol for the second one.

Fig. 3 shows the XRD patterns obtained for samples of the $Fe_{78.5}Ni_1Mo_{0.5}Si_6B_{14}$ alloy annealed up to different temperatures with

Table 1
Activation energy of primary and secondary crystallization determined for the examined amorphous alloys

Parameters	$Fe_{80}Si_6B_{14}$			$Fe_{78.5}Ni_1Mo_{0.5}Si_6B_{14}$		
Heating rate (K/min)	5	10	20	5	10	20
First peak (K)	771.9	779.9.6	795.1	780	783	795
Activation energy (kJ/mol)	380			440		
Second peak (K)	805.3	814.8	831.8	810	815	825
Activation energy (kJ/mol)	340			510		

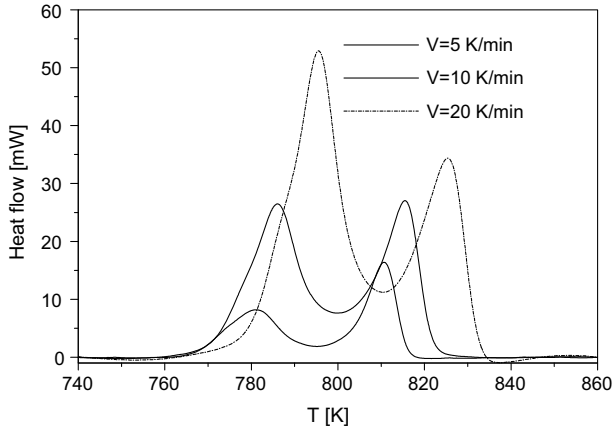

Fig. 1. DSC curves for the $Fe_{78.5}Ni_{1.0}Mo_{0.5}Si_{6.0}B_{14.0}$ amorphous alloy obtained for various heating rates.

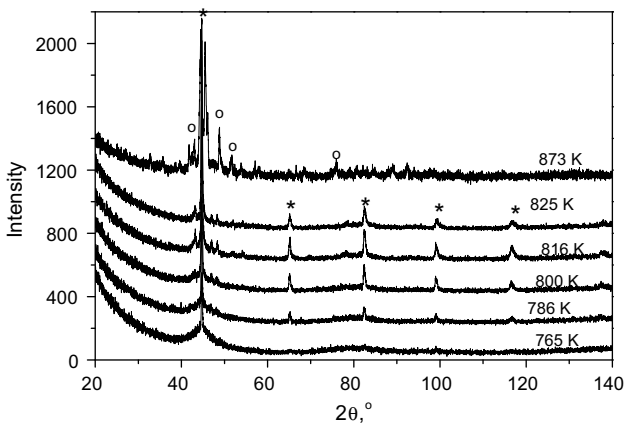

Fig. 3. XRD patterns obtained for samples of the $Fe_{78.5}Ni_1Mo_{0.5}Si_6B_{14}$ alloy annealed with heating rate 20 K/min up to different temperatures (α-Fe(Si) – *, Fe_2B – ○).

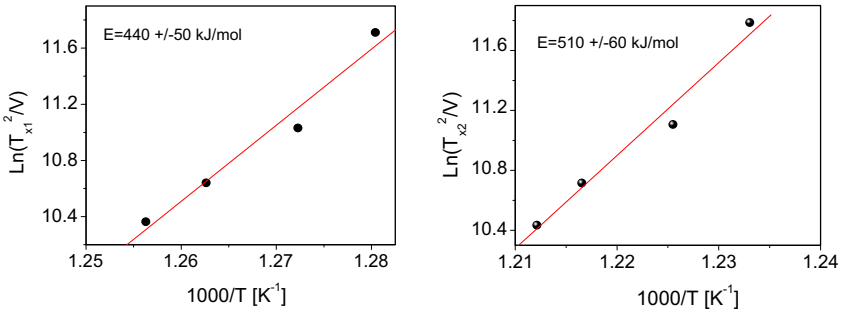

Fig. 2. Kissinger plot $\ln(T_x^2/V)$ vs $1000/T_x$ for the first and second exothermic DSC peaks for the $Fe_{78.5}Ni_1Mo_{0.5}Si_6B_{14}$ alloy (see Fig. 1).